

Over-Barrier Photoelectron emission with Rashba Spin-Orbit Coupling

Bi Hong Tiang,¹ Yee Sin Ang,^{1, a)} and L. K. Ang^{1, a)}

Science, Mathematics and Technology (SMT) Cluster, Singapore University of Technology and Design (SUTD), Singapore 487372

We develop a theoretical model to calculate the quantum efficiency (QE) of photoelectron emission from materials with Rashba spin-orbit coupling (RSOC) effect. In the low temperature limit, an analytical scaling between QE and the RSOC strength is obtained as $QE \propto (\hbar\omega - W)^2 + 2E_R(\hbar\omega - W) - E_R^2/3$, where $\hbar\omega$, W and E_R are the incident photon energy, work function and the RSOC parameter respectively. Intriguingly, the RSOC effect substantially improves the QE for strong RSOC materials. For example, the QE of Bi₂Se₃ and Bi/Si(111) increases, by 149% and 122%, respectively due to the presence of strong RSOC. By fitting to the photoelectron emission characteristics, the analytical scaling law can be employed to extract the RSOC strength, thus offering a useful tool to characterize the RSOC effect in materials. Importantly, when the traditional Fowler-Dubridge model is used, the extracted results may substantially deviate from the actual values by $\sim 90\%$, thus highlighting the importance of employing our model to analyse the photoelectron emission especially for materials with strong RSOC. These findings provide a theoretical foundation for the design of photoemitters using Rashba spintronic materials.

Photoemission¹ has significant technological applications in photoemission spectroscopy^{2,3}, x-ray generators⁴, and photodetectors⁵⁻⁹. One key property for studying photoelectron emission from materials is the quantum efficiency (QE), defined as the ratio of the number of emitted photo-electrons to the number of incident photons¹⁰. The prevailing method for determining QE in photoemission is based on the Fowler-Dubridge (FD) model^{11,12}, which was developed in the early twentieth century based on the assumption of a bulk material with parabolic energy dispersion. Multiple theoretical revisions of FD model have been subsequently developed, including the impact of laser heating on QE¹⁰, and generalized thermal-field-photoemission model¹³. Particularly, the use of quantum tunneling model have greatly enriches the photoemission physics over a wide range operating conditions to include various effects such as non-equilibrium heating at sub-ps time scale¹⁴, few cycles^{15,16}, consistent time-dependent tunneling model¹⁷⁻¹⁹, dielectric coating^{20,21}, and dual-lasers²².

These photoelectron emission models were however limited traditional metallic bulk materials that emerging nanomaterials, such as topological insulators^{23,24}, graphene^{25,26} and spintronic materials, are relatively studied if the FD model is valid. Unlike photoelectron emission, new models²⁷ for thermionic emission²⁸⁻³⁰ and field emission³¹⁻³³ models for novel materials have been developed.

Among the emerging materials, Rashba spintronic materials (RSM) have garnered significant attention due to their unique electronic properties, such as tunability³⁴⁻³⁷ and electronic band-splitting without an external magnetic field³⁸. RSM belong to a class of systems characterized by strong Rashba spin-orbit coupling^{39,40}, which was first proposed in 1959⁴¹. The Rashba effect results from the combination of spin-orbit interaction and breaking of inversion symmetry induced by an external electric field in a direction orthogonal to the two-dimensional material's surface. The Rashba effect has been studied and experimentally observed in various

materials, such as topological insulator Bi₂Se₃³⁶, metal⁴²⁻⁴⁴, graphene^{45,46}, InAlAs/InGaAs⁴⁷, BiTeI⁴⁸ and perovskite^{49,50}. The unique electronic structure of RSM can be harnessed to create spin-polarized currents^{51,52}, control the spin polarization and the direction of the spin currents⁵³. Thus, RSM are promising candidates for the development of spintronic devices, such as spin transistors⁵⁴ and spin-based memory devices⁵⁵.

Photoemission spectroscopy offers a valuable method for studying RSM. Specifically, the angle-resolved photoemission spectroscopy (ARPES) and the spin-resolved photoemission spectroscopy (SRPES) can be used to measure the Rashba splitting⁵⁶⁻⁶¹, to examine the spin-polarized photoemission^{60,61} and to investigate the electronic band structures of RSM^{62,63}. Consistent theoretical model for photoelectron emission for RSM remains limited and mostly bounded by the classic FD model, which does not include the spins splitting effects in the formulation. For instance, ARPES and SRPES utilize the assumption of parabolic electron dispersion to estimate the Rashba parameter α_R based on the values of measured momentum offset $k_0 = \alpha_R m / \hbar^2$ and Rashba energy $E_R = \hbar^2 k_0^2 / 2m$. Such approach has, however, overlooked the spin splitting within the dispersion and may introduce errors in the estimation of the Rashba parameter⁴⁸.

In this work, we develop a theoretical model to study how the Rashba spin-orbit coupling (RSOC) will modify the quantum efficiency (QE) of photoelectron emission from Rashba spintronic materials (RSM). In low temperature limit, our model presents an analytical scaling of $QE \propto (\hbar\omega - W)^2 + 2E_R(\hbar\omega - W) - E_R^2/3$, where $\hbar\omega$, W and E_R are the incident photon energy, work function and the RSOC parameter respectively. This finding suggest that the traditional Fowler-Dubridge (FD) model is no longer valid for photoelectron emission for RSM. Our model reveals that RSOC substantially increase the QE for materials with a strong RSOC strength and photon energy close to an effective work function ($W + E_R$). For instance, QE of Bi₂Se₃ increases by up to 95% due to the presence of strong RSOC. Substantial error appears if the traditional FD model is used to characterize the photoelectron emission from RSM in order to estimate its RSOC strength.

^{a)} Authors to whom correspondence should be addressed: yeesin_ang@sutd.edu.sg and ricky_ang@sutd.edu.sg

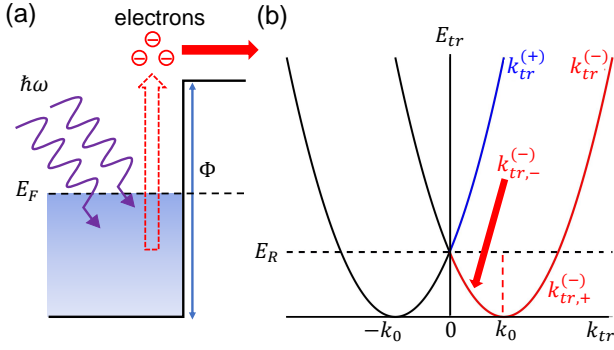


FIG. 1. Schematic diagrams of (a) the over-barrier photoemission; and (b) the electron energy dispersion of a Rashba spintronic materials plotted with $k_{inj} = 0$. The notation \pm corresponds to the electronic band $s = \pm 1$.

First, the QE of photoemission in the FD model is¹⁸

$$QE = a_1(1-r)A_1T^2F\left(\frac{\hbar\omega - W}{k_B T}\right), \quad (1)$$

where the QE is a function of incident photon energy $\hbar\omega$, material's work function W and temperature T . Refer to Eq. (5) for the detailed explanation of Eq. (1) and the defined parameters. In our derivation, we employ the FD approach to derive its QE, but replace the standard parabolic electron dispersion with the proper dispersion of RSM as shown in Eq. (3). Assuming the incident photon is in z -direction and the electrons obey Fermi-Dirac distribution, the QE of photoelectron emis-

sion is calculated by

$$QE \propto \frac{g}{(2\pi)^3} \int d\phi \int dk_{tr} k_{tr} \int dk_z \frac{\Theta[E_{inj} - (E_F + W - \hbar\omega)]}{\exp[(E_{tr} + E_{inj} - E_F)/k_B T] + 1} \quad (2)$$

where g is the degeneracy of electron's states, E_F is the Fermi energy, W is work function, $\hbar\omega$ is the injected photon energy, k_B is the Boltzmann constant, $\Theta[E_{inj} - (E_F + W - \hbar\omega)]$ is the Heaviside electron tunneling probability as the amount of energy required to overcome the barrier is reduced by the amount of injected photon energy [see Fig. 1(a)]. Based on the Rashba's system dispersion³⁸, we have

$$E_{k,s} = \underbrace{\frac{\hbar^2}{2m} [(k_{tr} + sk_0)^2]}_{E_{tr}} + \underbrace{\left[\frac{\hbar^2}{2m} k_z^2 \right]}_{E_{inj}} \quad (3)$$

where $E_{k,s}$ is the total energy, $k_0 = \alpha_R m / \hbar^2$ is the material-dependent parameter associated with the RSOC strength α_R , m is the electron effective mass m and \hbar reduced Planck's constant. Here, E_{tr} and E_{inj} is the energy in xy -plane and z -direction, respectively, $s = \pm 1$ corresponds to different electronic conduction band, $\vec{k} = (k_x, k_y, k_z)$ is the wave vector, and $k_{tr} = \sqrt{k_x^2 + k_y^2}$.

To solve Eq. (2), we determine the real solution of $k_{tr}^{(s)} \geq 0$ in the Rashba dispersion as indicated in Fig. 1(b). Let's define the Rashba energy as $E_R = \hbar^2 k_0^2 / 2m$. At $s = +1$, we only have $k_{tr}^{(+)} = \sqrt{2mE_{tr}}/\hbar - k_0$ for $E_{tr} \geq E_R$. At $s = -1$, we obtain $k_{tr,\eta}^{(-)} = \eta\sqrt{2mE_{tr}}/\hbar + k_0$ for $E_{tr} \leq E_R$ where $\eta = \pm 1$, and $k_{tr}^{(-)} = \sqrt{2mE_{tr}}/\hbar + k_0$ for $E_{tr} \geq E_R$. Thus, Eq. (2) becomes

$$QE \propto \frac{1}{2\sqrt{2}\pi^2} \frac{m^{3/2}}{\hbar^3} \left\{ \int_{E_F+W-\hbar\omega}^{\infty} \frac{dE_{inj}}{\sqrt{E_{inj}}} \int_{E_R}^{\infty} dE_{tr} f_{FD} + \frac{\hbar k_0}{\sqrt{2m}} \int_0^{E_R} \frac{dE_{tr}}{\sqrt{E_{tr}}} \int_{E_F+W-\hbar\omega}^{\infty} dE_{inj} \frac{f_{FD}}{\sqrt{E_{inj}}} \right\} \quad (4)$$

where $f_{FD} = \frac{1}{\exp[(E_{tr} + E_{inj} - E_F)/k_B T] + 1}$ denotes the Fermi-Dirac distribution. Note Equation. (4) can be rewritten as

$$QE = a_1(1-r)A_1T^2 \left[F\left(\frac{\hbar\omega - W - E_R}{k_B T}\right) + 2\sqrt{\frac{E_R}{k_B T}} \mathcal{R}(\hbar\omega, W, E_R, k_B T) \right] \quad (5)$$

, where an experimental fitting parameter a_1 (like in the FD model) has been added. For example, $a_1 = 5 \times 10^{-18} \text{ m}^2/\text{A}$ for Cu¹⁸. Here the parameter r is the reflectivity which depends on the incident photon wavelength, angle, and refractive index of the materials. The constant $A_1 = 120 \text{ A}/(\text{cm}^2 \text{K}^2)$ is the Richardson's constant. The two functions are the Fowler function $F(x) = \pi^2/6 + x^2/2 - \exp(-x) + \exp(-2x)/2^2 + \dots$ for $x > 0$ ^{11,18}, and a new normalized function of

$$\mathcal{R}(\hbar\omega, W, E_R, k_B T) = \int_0^{\sqrt{E_R/k_B T}} du \ln \left[1 + \exp\left(\frac{\hbar\omega - W}{k_B T} - u^2\right) \right]. \quad (6)$$

We recover Eq. (1) from Eq. (5) at $E_R = 0$ and thus converges to the FD model without RSOC for consistency purpose.

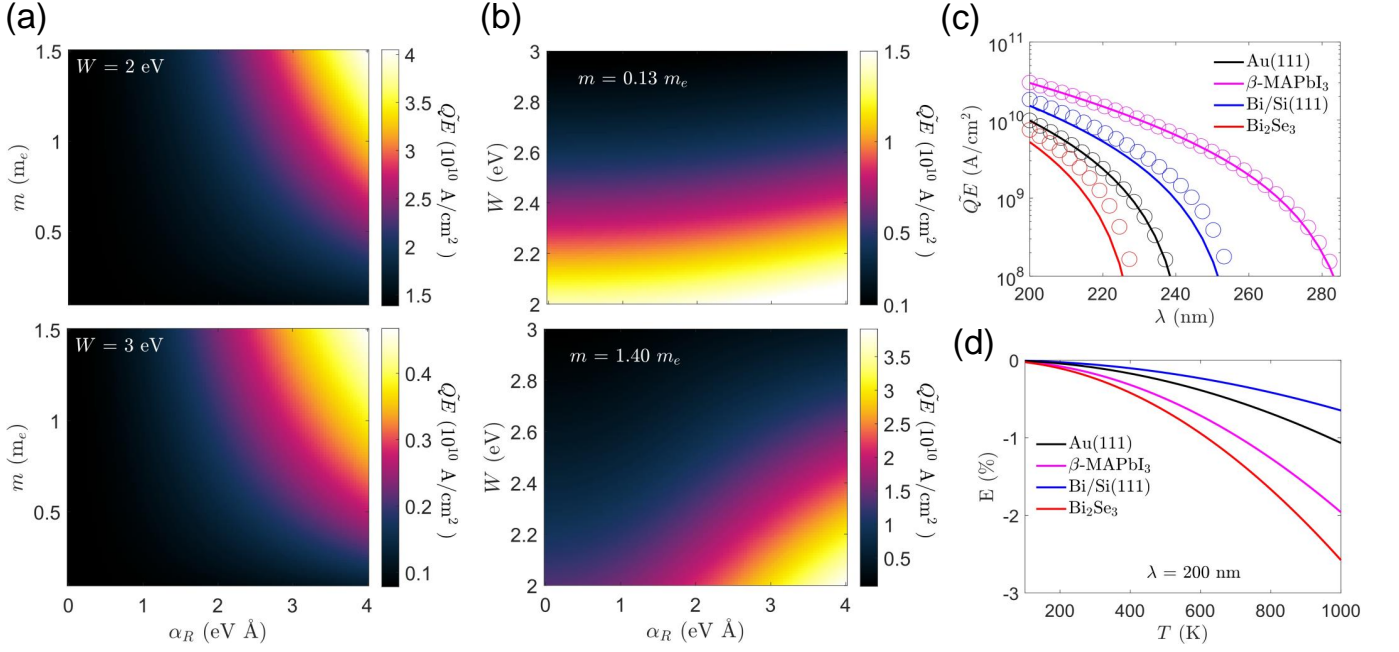


FIG. 2. QE enhancement due to Rashba spin-orbit coupling effect (RSOC) at temperature $T = 300$ K. (a) The $\tilde{Q}E \equiv QE/a_1(1-r)$ as a function of electron effective mass (m) and RSOC strength (α_R) is calculated for work functions $W = 2$ eV (top) and $W = 3$ eV (bottom). (b) The $\tilde{Q}E$ as a function of work function (W) and RSOC strength (α_R) is calculated for electron effective masses $m = 0.13 m_e$ (top); and $m = 1.40 m_e$ (bottom). The incident light wavelength is set to a representative value of $\lambda = 375$ nm. (c) The $\tilde{Q}E$ as a function of laser wavelength λ for different materials: $\tilde{Q}E$ without RSOC (solid line) and $\tilde{Q}E$ with RSOC (circle). (d) $E = [QE(T \rightarrow 0) - QE]/QE$ as a function of temperature (T), where E is the relative error percentage between the numerical solution of $\tilde{Q}E$ at T up to 1000 K and the analytical $\tilde{Q}E$ based on $T=0$ approximation.

The RSOC effect or finite value of E_R has two effects. Firstly, it raises the effective work function of the first term in Eq.(5) from W to $W + E_R$. The second term in Eq. (5) serves the enhancement of QE due to finite E_R . Thus, the net effect of RSOC will depend on the laser wavelength, material's work function, temperature and RSOC strength as shown in the figures below. At low temperature limit $k_B T \ll \hbar\omega - W - E_R$ [see Supplementary materials (SM) for the complete derivation], Eq. (5) can be further simplified to an analytical form of

$$QE(T \rightarrow 0) = \Theta(\hbar\omega - W - E_R) \frac{a_1(1-r)A_1}{2k_B^2} \left[(\hbar\omega - W)^2 + 2E_R(\hbar\omega - W) - E_R^2/3 \right], \quad (7)$$

where $\Theta(x)$ is the Heaviside function. From Fig. 2(f), Eq. (7) agrees well with Eq. (5) at room temperature $T = 300$ K and wavelength $\lambda = 200$ nm as the error E is less than 1 %. However, when the wavelength or temperature increases, the error E also increases. Thus, Eq. (7) is a good approximation only when the ratio $\left(\frac{\hbar\omega - W - E_R}{k_B T}\right)$ is large. Importantly, the experimental fitting of Eq. (7) allows for the determination of the work function W and parameter E_R , which play a crucial role in characterizing the fundamental features of Rashba spintronic materials.

TABLE I. Physical properties of selected materials.

Materials	W (eV)	E_R (meV)	α_R (eV Å)	m (m_e)
Au (111)	5.1 ¹⁸	2.1 ⁴⁸	0.33 ⁴⁸	0.29
β -MAPbI ₃	4.28 ⁶⁴	12 ⁶⁵	1.5 ⁶⁵	0.10
Bi/Si(111)	4.83 ⁶⁶	140 ⁶⁷	1.37 ⁶⁷	1.14
Bi ₂ Se ₃	5.4 ⁶⁸	180 ⁶⁹	4.0 ³⁹	0.17

The FD model suggests a dependence of $QE \propto (\hbar\omega - W)^2$

which agrees well with experimental data²⁷. Here, Eq. (7) generalizes the QE of a photoemitter to the case of Rashba spintronic system, yielding an unconventional scaling of

$$QE \propto (\hbar\omega - W)^2 + 2E_R(\hbar\omega - W) - E_R^2/3. \quad (8)$$

To analyze the parametric dependence of photoemission QE in RSM, we numerically compute the QE for different set of physical parameters, including electron effective mass, work function, laser wavelength, temperature and RSOC strength [see Fig. (2) and Fig. (3)]. In Fig. 2, we plot $\tilde{Q}E \equiv QE/a_1(1-r)$ as a_1 and r are some material-dependent param-

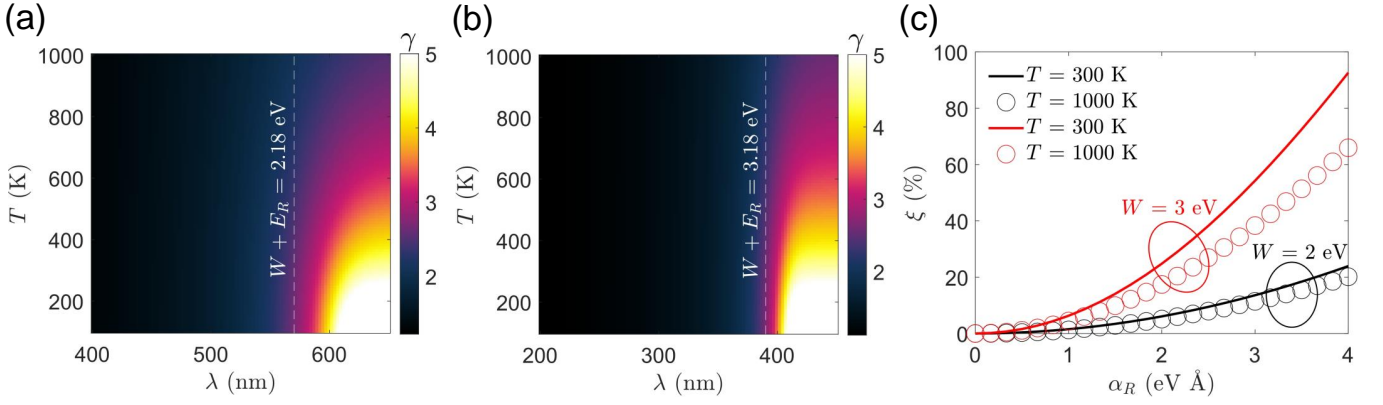


FIG. 3. The effect of work function and incident laser wavelength in photoemission enhancement due to Rashba spin-orbit coupling (RSOC) effect. Here, we employ the values of electron effective mass and RSOC strength of Bi_2Se_3 . γ is the enhancement due to RSOC as a function of laser wavelength (λ) and temperature (T) for work function (a) $W = 2$ eV; and (b) $W = 3$ eV. The white dashed line indicates the incident wavelength corresponds to the threshold $W + E_R$. (c) The relative error ξ as a function of RSOC strength (α_R) at different temperature $T = 300$ K (solid line), 1000 K (circle) and laser wavelength $\lambda = 375$ nm for work function $W = 2$ eV (black) and $W = 3$ eV (red).

eters, which may be determined experimentally. For both low and high work function case [see Fig. 2(a)], we observe that increasing the electron effective mass m or RSOC strength α_R will lead to an increase in QE. Figure 2(b) show that a higher electron effective mass (m) will imply a more pronounced enhancement of $\tilde{Q}E$, owing to the m -dependence of E_R . Since both the electron effective mass m and RSOC strength α_R are positively correlated with E_R , increasing E_R will lead to an increase in $\tilde{Q}E$. Moreover, as depicted in Fig. 2(a,b), $\tilde{Q}E$ decreases with higher work function W as expected as fewer electrons possess adequate energy to overcome the higher W .

In Fig. 2(c), we specifically pick four materials with different E_R as shown in Table. (I): Au(111), β -MAPbI₃, Bi/Si(111) and Bi_2Se_3 . The calculated results in the figure compare the calculations with (symbols) and without the RSOC effect. The comparison suggests significant difference for Bi/Si(111) and Bi_2Se_3 due to larger values of E_R for both materials. The figure also shows that the $\tilde{Q}E$ improvement is more significant at longer wavelengths.

To study the wavelength dependence of QE improvement, we compute the ratio of QE with RSOC to the QE without RSOC (γ), i.e.

$$\gamma = \frac{F\left(\frac{\hbar\omega - W - E_R}{k_B T}\right) + 2\sqrt{\frac{E_R}{k_B T}}\mathcal{R}(\hbar\omega, W, E_R, k_B T)}{F\left(\frac{\hbar\omega - W}{k_B T}\right)} \quad (9)$$

where the functions F , \mathcal{R} and parameter B_1 are defined in Eq. (5). For over-barrier photoemission $\hbar\omega \geq W + E_R$, Fig. 3 (a,b) reveals that the presence of strong Rashba spin-orbit coupling (RSOC) results in a QE enhancement ranging from approximately 15% to 150%. The QE enhancement rises at longer laser wavelength, which is consistent with Fig. 2(c). For laser energies lower than the threshold of $W + E_R$, Fig. 3 (a,b) predicts a huge QE enhancement, estimated to be at least $\sim 150\%$. There is also a significant decrease in the QE enhancement as the temperature increases, suggesting that ther-

mal excitation has emerged as a crucial factor affecting QE enhancement. Hence, in both low and high photon energy scenarios, RSOC presents a compelling opportunity to boost the QE of electron emission.

Finally, for photoemission experiment, the value of the prefactor a_1 is fitted by measuring QE. Here, we estimate the relative error percentage ξ for the values of a_1 extracted via the traditional FD model ($a_1^{(FD)}$) and our model ($a_1^{(R)}$), in which the ξ is given by

$$\xi = \frac{a_1^{(FD)} - a_1^{(R)}}{a_1^{(R)}} = \gamma - 1 \quad (10)$$

where γ is defined in Eq. (9). Figure 3(c) shows that ξ will increase with RSOC strength. The error is also more significant at lower temperature and higher work function. As an example, the peak $\xi = 90\%$ occurs at work function $W = 3$ eV, $T = 300$ K and RSOC strength $\alpha_R = 4$ eV \AA . This discrepancy in extracted values of the a_1 parameter between our model and Fowler-Dubridge model is significant, and hence emphasizing the importance of using the appropriate model when examining photoemission measurement data. Furthermore, when the laser energy approaches the threshold of $W + E_R$, an increase in temperature will cause in a notable decrease in the values of ξ as depicted in Fig. 3(c), which suggests the impact of RSOC on QE diminishing at higher temperatures. Thus, our results predicts a substantial QE improvement at low temperature (room temperature) for materials with a strong RSOC strength and for incident photon energy near the threshold $W + E_R$. Conversely, materials with a weak RSOC strength or high incident photon energy exceeding the $W + E_R$ threshold exhibit a low QE enhancement. Our model can facilitate the design of high-performance photodetectors by tuning the RSOC strength³⁴⁻³⁷ to advance both fundamental knowledge and applications.

In summary, we have developed a theoretical model to calculate the quantum efficiency (QE) of photoelectron emission from Rashba spintronic materials with RSOC effect. In low

temperature limit [see Eq. (7)], our model presents an analytical expression of $QE \propto (\hbar\omega - W)^2 + 2E_R(\hbar\omega - W) - E_R^2/3$, where $\hbar\omega$, W and E_R are the incident photon energy, work function and the RSOC parameter respectively. This unique scaling law can be conveniently employed to gauge the RSOC strength in RSM, thus providing a useful tool for characterizing Rashba spintronic materials. Importantly, RSOC substantially improves the QE for materials with a strong RSOC strength and for photon energy close to an effective work function ($W + E_R$) [see Fig. 3(a,b)]. For instance, QE of Bi_2Se_3 increases by up to 149% and QE of $\text{Bi/Si}(111)$ increases by up to 122% , due to the presence of strong RSOC.

It is essential to employ our proposed model here to examine photoelectron emission data as the prefactor a_1 parameter from the traditional Fowler-Dubridge (FD) model can substantially deviate from the actual values up to 90% [see Fig. 3(c)]. These findings pave the way for the advancement and characterization of photodetectors that rely on Rashba spintronic materials. For future works, the formulation in this work is limited to a specific range of incident photon wavelengths, where the photon energy is greater than the work function of the materials, where the single-photon absorption dominates the photoemission process¹⁸. The model can be expanded to include multiphoton absorption and optical tunneling regimes by considering longer incident photon wavelengths.

See supplementary material for the complete derivation of Eq. (7).

ACKNOWLEDGEMENTS

This work is supported by the Singapore A*STAR IRG grant (A2083c0057). Y. S. A. is supported by the Singapore Ministry of Education Academic Research Fund Tier 2 (Award No. MOE-T2EP50221-0019)

AUTHOR DECLARATIONS

CONFLICT OF INTEREST

The authors have no conflicts to disclose.

AUTHOR CONTRIBUTIONS

Bi Hong Tiang: Methodology (equal), Investigation (lead), Writing - Original Draft (lead). **Lay Kee Ang:** Conceptualization (lead), Supervision (equal), Writing - Review & Editing (equal). **Yee Sin Ang:** Methodology (equal), Supervision (lead), Writing - Review & Editing (lead).

DATA AVAILABILITY

The data that support the findings of this study are available from the corresponding author upon reasonable request.

- ¹A. Pais, *Rev. Mod. Phys.* **51**, 863 (1979).
- ²A. Damascelli, *Physica Scripta* **2004**, 61 (2004).
- ³A. Damascelli, Z. Hussain, and Z.-X. Shen, *Rev. Mod. Phys.* **75**, 473 (2003).
- ⁴R. J. England, R. J. Noble, K. Bane, D. H. Dowell, C.-K. Ng, J. E. Spencer, S. Tantawi, Z. Wu, R. L. Byer, E. Peralta, K. Soong, C.-M. Chang, B. Montazeri, S. J. Wolf, B. Cowan, J. Dawson, W. Gai, P. Hommelhoff, Y.-C. Huang, C. Jing, C. McGuinness, R. B. Palmer, B. Naranjo, J. Rosenzweig, G. Travish, A. Mizrahi, L. Schachter, C. Sears, G. R. Werner, and R. B. Yoder, *Rev. Mod. Phys.* **86**, 1337 (2014).
- ⁵J. Wu, S. Chen, A. Seeds, and H. Liu, *Journal of Physics D: Applied Physics* **48**, 363001 (2015).
- ⁶Z. Zhang, B. Cheng, J. Lim, A. Gao, L. Lyu, T. Cao, S. Wang, Z.-A. Li, Q. Wu, L. K. Ang, *et al.*, *Advanced Materials*, 2206196 (2022).
- ⁷W. Lei and C. Jagadish, *Journal of Applied Physics* **104**, 11 (2008).
- ⁸E. M. Gallo, G. Chen, M. Currie, T. McGuckin, P. Prete, N. Lovergine, B. Nabet, and J. E. Spanier, *Applied Physics Letters* **98**, 241113 (2011).
- ⁹T. Mueller, F. Xia, and P. Avouris, *Nature photonics* **4**, 297 (2010).
- ¹⁰Y. Zhou and P. Zhang, *Journal of Applied Physics* **130**, 064902 (2021).
- ¹¹R. H. Fowler, *Phys. Rev.* **38**, 45 (1931).
- ¹²L. A. DuBridge, *Phys. Rev.* **39**, 108 (1932).
- ¹³K. L. Jensen, P. G. O'Shea, and D. W. Feldman, *Applied physics letters* **81**, 3867 (2002).
- ¹⁴L. Wu and L. K. Ang, *Phys. Rev. B* **78**, 224112 (2008).
- ¹⁵M. Pant and L. K. Ang, *Phys. Rev. B* **86**, 045423 (2012).
- ¹⁶Y. Luo, Y. Zhou, and P. Zhang, *Phys. Rev. B* **103**, 085410 (2021).
- ¹⁷M. Pant and L. K. Ang, *Phys. Rev. B* **88**, 195434 (2013).
- ¹⁸Y. Zhou and P. Zhang, *Journal of Applied Physics* **127**, 164903 (2020).
- ¹⁹P. Zhang and Y. Lau, *Scientific reports* **6**, 1 (2016).
- ²⁰X. Xiong, Y. Zhou, Y. Luo, X. Li, M. Bosman, L. K. Ang, P. Zhang, and L. Wu, *ACS Nano* **14**, 8806 (2020).
- ²¹Y. Zhou and P. Zhang, *Journal of Applied Physics* **131**, 064903 (2022).
- ²²Y. Luo and P. Zhang, *Phys. Rev. B* **98**, 165442 (2018).
- ²³D. Hsieh, Y. Xia, D. Qian, L. Wray, J. Dil, F. Meier, J. Osterwalder, L. Patthey, J. Checkelsky, N. P. Ong, *et al.*, *Nature* **460**, 1101 (2009).
- ²⁴M. Z. Hasan and C. L. Kane, *Rev. Mod. Phys.* **82**, 3045 (2010).
- ²⁵E. Krasovskii, *Nanomaterials* **11** (2021), 10.3390/nano11051212.
- ²⁶P. Ayria, A. R. T. Nugraha, E. H. Hasdeo, T. R. Czank, S.-i. Tanaka, and R. Saito, *Phys. Rev. B* **92**, 195148 (2015).
- ²⁷Y. S. Ang, L. Cao, and L. K. Ang, *InfoMat* **3**, 502 (2021).
- ²⁸S.-J. Liang and L. K. Ang, *Phys. Rev. Appl.* **3**, 014002 (2015).
- ²⁹Y. S. Ang, H. Y. Yang, and L. K. Ang, *Phys. Rev. Lett.* **121**, 056802 (2018).
- ³⁰Y. S. Ang, Y. Chen, C. Tan, and L. K. Ang, *Phys. Rev. Appl.* **12**, 014057 (2019).
- ³¹W. J. Chan, Y. S. Ang, and L. K. Ang, *Phys. Rev. B* **104**, 245420 (2021).
- ³²C. Chua, C. Y. Kee, Y. S. Ang, and L. Ang, *Phys. Rev. Appl.* **16**, 064025 (2021).
- ³³L. K. Ang, Y. S. Ang, and C. H. Lee, *Physics of Plasmas* **30**, 033103 (2023).
- ³⁴Q. Liu, Y. Guo, and A. J. Freeman, *Nano letters* **13**, 5264 (2013).
- ³⁵S. Singh and A. H. Romero, *Phys. Rev. B* **95**, 165444 (2017).
- ³⁶P. D. C. King, R. C. Hatch, M. Bianchi, R. Ovsyannikov, C. Lupulescu, G. Landolt, B. Slomski, J. H. Dil, D. Guan, J. L. Mi, E. D. L. Rienks, J. Fink, A. Lindblad, S. Svensson, S. Bao, G. Balakrishnan, B. B. Iversen, J. Osterwalder, W. Eberhardt, F. Baumberger, and P. Hofmann, *Phys. Rev. Lett.* **107**, 096802 (2011).
- ³⁷A. D. Caviglia, M. Gabay, S. Gariglio, N. Reyren, C. Cancellieri, and J.-M. Triscone, *Phys. Rev. Lett.* **104**, 126803 (2010).
- ³⁸Z.-G. Yu, *Phys. Chem. Chem. Phys.* **19**, 14907 (2017).
- ³⁹A. Manchon, H. C. Koo, J. Nitta, S. M. Frolov, and R. A. Duine, *Nature materials* **14**, 871 (2015).
- ⁴⁰G. Bihlmayer, P. Noël, D. V. Vyalikh, E. V. Chulkov, and A. Manchon, *Nature Reviews Physics* **4**, 642 (2022).
- ⁴¹E. RASHBA, *Sov. Phys.-Solid State* **2**, 1109 (1960).
- ⁴²A. Nuber, J. Braun, F. Forster, J. Minár, F. Reinert, and H. Ebert, *Phys. Rev. B* **83**, 165401 (2011).
- ⁴³A. Varykhalov, D. Marchenko, M. R. Scholz, E. D. L. Rienks, T. K. Kim, G. Bihlmayer, J. Sánchez-Barriga, and O. Rader, *Phys. Rev. Lett.* **108**, 066804 (2012).
- ⁴⁴F. Meier, H. Dil, J. Lobo-Checa, L. Patthey, and J. Osterwalder, *Phys. Rev. B* **77**, 165431 (2008).

- ⁴⁵H. Min, J. E. Hill, N. A. Sinitsyn, B. R. Sahu, L. Kleinman, and A. H. MacDonald, *Phys. Rev. B* **74**, 165310 (2006).
- ⁴⁶D. Marchenko, A. Varykhalov, M. Scholz, G. Bihlmayer, E. Rashba, A. Rybkin, A. Shikin, and O. Rader, *Nature communications* **3**, 1232 (2012).
- ⁴⁷J. Nitta, T. Akazaki, H. Takayanagi, and T. Enoki, *Phys. Rev. Lett.* **78**, 1335 (1997).
- ⁴⁸K. Ishizaka, M. Bahramy, H. Murakawa, M. Sakano, T. Shimojima, T. Sonobe, K. Koizumi, S. Shin, H. Miyahara, A. Kimura, *et al.*, *Nature materials* **10**, 521 (2011).
- ⁴⁹M. Kim, J. Im, A. J. Freeman, J. Ihm, and H. Jin, *Proceedings of the National Academy of Sciences* **111**, 6900 (2014).
- ⁵⁰S. B. Todd, D. B. Riley, A. Binai-Motlagh, C. Clegg, A. Ramachandran, S. A. March, J. M. Hoffman, I. G. Hill, C. C. Stoumpos, M. G. Kanatzidis, *et al.*, *APL Materials* **7**, 081116 (2019).
- ⁵¹A. Manchon, H. Koo, J. Nitta, S. Frolov, and R. Duine, *Nature materials* **14** (2015), 10.1038/nmat4360.
- ⁵²B. Dieny, I. L. Prejbeanu, K. Garello, P. Gambardella, P. Freitas, R. Lehn-dorff, W. Raberg, U. Ebels, S. O. Demokritov, J. Akerman, *et al.*, *Nature Electronics* **3**, 446 (2020).
- ⁵³T. Koga, J. Nitta, H. Takayanagi, and S. Datta, *Phys. Rev. Lett.* **88**, 126601 (2002).
- ⁵⁴I. Žutić, J. Fabian, and S. Das Sarma, *Rev. Mod. Phys.* **76**, 323 (2004).
- ⁵⁵J. Puebla, J. Kim, K. Kondou, and Y. Otani, *Communications Materials* **1**, 24 (2020).
- ⁵⁶K. Yaji, Y. Ohtsubo, S. Hatta, H. Okuyama, K. Miyamoto, T. Okuda, A. Kimura, H. Namatame, M. Taniguchi, and T. Aruga, *Nature communications* **1**, 17 (2010).
- ⁵⁷J.-H. Park, C. H. Kim, J.-W. Rhim, and J. H. Han, *Phys. Rev. B* **85**, 195401 (2012).
- ⁵⁸Y. S. Dedkov, M. Fonin, U. Rüdiger, and C. Laubschat, *Phys. Rev. Lett.* **100**, 107602 (2008).
- ⁵⁹S. LaShell, B. A. McDougall, and E. Jensen, *Phys. Rev. Lett.* **77**, 3419 (1996).
- ⁶⁰F. Meier, J. H. Dil, and J. Osterwalder, *New Journal of Physics* **11**, 125008 (2009).
- ⁶¹U. Heinzmann and J. H. Dil, *Journal of Physics: Condensed Matter* **24**, 173001 (2012).
- ⁶²T. Okuda and A. Kimura, *Journal of the Physical Society of Japan* **82**, 021002 (2013).
- ⁶³T. Okuda, *Journal of Physics: Condensed Matter* **29**, 483001 (2017).
- ⁶⁴Y. Miao, X. Wang, H. Zhang, T. Zhang, N. Wei, X. Liu, Y. Chen, J. Chen, and Y. Zhao, *eScience* **1**, 91 (2021).
- ⁶⁵M. Kim, J. Im, A. J. Freeman, J. Ihm, and H. Jin, *Proceedings of the National Academy of Sciences* **111**, 6900 (2014).
- ⁶⁶F. G. Allen and G. W. Gobeli, *Phys. Rev.* **127**, 150 (1962).
- ⁶⁷I. Gierz, T. Suzuki, E. Frantzeskakis, S. Pons, S. Ostanin, A. Ernst, J. Henk, M. Grioni, K. Kern, and C. Ast, *Physical review letters* **103**, 046803 (2009).
- ⁶⁸M. T. Edmonds, J. T. Hellerstedt, A. Tadich, A. Schenk, K. M. O'Donnell, J. Tosado, N. P. Butch, P. Syers, J. Paglione, and M. S. Fuhrer, *The Journal of Physical Chemistry C* **118**, 20413 (2014).
- ⁶⁹P. D. C. King, R. C. Hatch, M. Bianchi, R. Ovsyannikov, C. Lupulescu, G. Landolt, B. Slomski, J. H. Dil, D. Guan, J. L. Mi, E. D. L. Rienks, J. Fink, A. Lindblad, S. Svensson, S. Bao, G. Balakrishnan, B. B. Iversen, J. Osterwalder, W. Eberhardt, F. Baumberger, and P. Hofmann, *Phys. Rev. Lett.* **107**, 096802 (2011).